Modeling and Predicting Visual Outcomes With VOL-3D

Edwin J. Sarver, PhD; Raymond A. Applegate, OD, PhD

Modeling the optics of the eye, and in particular the optics of an individual patient's eye, and predicting the resulting visual performance are major goals of visual optics and clinical researchers. The benefits of obtaining these goals include designing new optical corrections, selecting the best available correction to meet a particular patient's needs, and demonstrating to the patient likely outcomes of various interventions.

We report here our progress in developing a program called Visual Optics Lab – 3D (VOL-3D). The overall goal of the project is to develop for clinical and research use, a user-friendly software program that models and evaluates the optics of a real and/or user defined eye and stores analysis outcomes in a relational database. In developing the program, we followed the same fundamental analysis path as Greivenkamp and colleagues[1], by constructing an optical model for an individual eye and applying ray-tracing analysis to the composite model. Our techniques go further in that we integrate all the various software functions required to construct a model and analyze its performance into a single program using units and terms familiar to the ophthalmic and visual optics community. In this paper we demonstrate the methods employed by VOL-3D by building an eye model using a combination of clinical and schematic eye data. We then optically correct the eye using various modes of correction and evaluate and compare the optical performance of each correction mode.

From Sarver and Associates, Inc., Merritt Island, FL (Sarver) and the Department of Ophthalmology, University of Texas Health Science Center at San Antonio, San Antonio, TX (Applegate).

Funding support for this work was provided by NEI R43 EY11681 to EJS and R01 EY08520 to RAA and an unrestricted grant to the Department of Ophthalmology from Research to Prevent Blindness, NY, NY.

The authors have a commercial interest in Visual Optics Lab-3D (VOL-3D).

Correspondence: Edwin J. Sarver, PhD, Sarver and Associates, Inc., 3425 Savannahs Trail, Merritt Island, FL 32953. Tel: 321.452.2639; Fax: 321.452.7210; E-mail: ejsarver@VOL3D.com

MATERIALS AND METHODS

For demonstration purposes we constructed a model eye using clinical examination data derived from corneal topography and fill in missing or unavailable data with the parameters of a state-of-the-art schematic eye. To correct the optical defects of the eye, we incorporated into the model, one at a time, a variety of different compensating optics including: a spectacle lens, contact lens, a modified corneal surface, and a phakic intraocular lens (IOL). Forms for the compensating optic included sphere, sphero-cylinder, and higher-order surfaces such as a b-spline or Zernike polynomial expansion. To simulate visual performance and evaluate the optical quality of each model eye and its correction, we generated simulated retinal images, wavefront aberration maps and tables, point spread functions, spot diagrams, modulation transfer functions, and merit function values (eg, Stiles-Crawford root mean square [RMS] spot size (SC-RMS), Strehl ratio, area under the two-dimensional modulation transfer function [MTF], etc.). In this manner several different modes of correction were tested and compared to determine the best choice of correction.

VOL-3D provides standard schematic eye models and the ability to start from scratch and build and place each surface individually (in x, y and z as well as tilted) within the model. For convenience, we began our eye model construction using the parameters of the four-surface, aspheric Schwiegerling schematic eye model[2] that are given in Table 1. It is easier to start with a defined schematic eye and substitute or change surfaces than it is to build a model from scratch. In the model we present here, we substitute for the conic surface of the anterior cornea of the Schwiegerling model a b-spline surface fit to corneal topography from a commercially available system. The program supports the input of most commonly used corneal topography units. To review the corneal topography examination, the program provides several displays including: axial color map, elevation map relative to a plane, elevation map

Table 1
Parameters for Schwiegerling Four-surface Schematic Eye

Surface	Radius (mm)	Conic, p	Thickness (mm)	Index
Anterior cornea	7.8	0.75	0.55	1.3771
Posterior cornea	6.5	0.75	3.05	1.3374
Anterior lens	11.03	-3.30	4.0	1.42
Posterior lens	-5.72	-1.17	16.6	1.336

relative to a conic, wavefront error color map, and wavefront error for a user specified set of Zernike polynomial expansion terms of any reference surface of interest (Figs 1-3). A particularly interesting reference surface, assuming proper registration can be achieved, is the corneal surface designed to reduce the aberration structure of the eye.

As seen in Figure 1, the axial topography display reveals that the corneal first surface we wish to add to our model eye has about 2.30 diopters (D) of

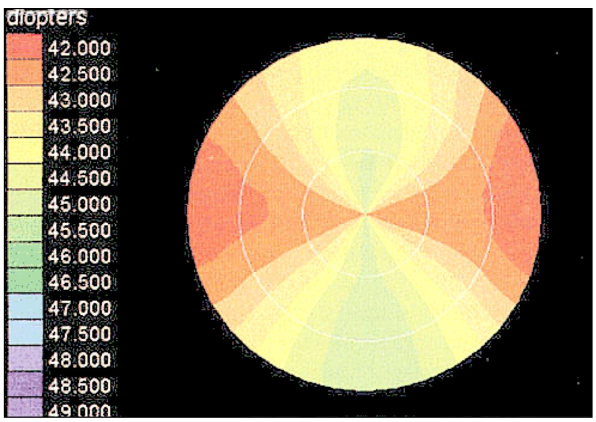

Figure 1. Axial map of human eye corneal topography examination from a commercial system.

slightly asymmetric, with-the-rule astigmatism. In Table 2 we show the results of computing the corneal first surface wavefront error with respect to a best focus reference sphere for the optics of the corneal first surface. The sum of the coefficient variances are given in column 5 of this table; 94% of the corneal wavefront error variance is contained in the single term corresponding to astigmatism and the remaining 6% is distributed in the remainder of the terms. Illustrated in Figure 3 is the effect of including the astigmatic term (3A) and removing the astigmatic term (3B and 3C) from the corneal first surface wavefront error (in waves at 555 nm) for a 6.0 mm pupil. Removing the astigmatic term and adjusting the sensitivity of the scale allows one to see the higher order aberrations in 3C masked by the sphere and/or cylinder error in 3A.

Replacing the model eye's corneal surface with an optical surface generated from corneal topography data will change the model's conventional refractive and higher order aberration structure (unless of course it was identical to the original model surface). As much clinical data as is available (eg, corneal back surface topography, corneal thickness, anterior chamber depth, axial length, etc.) can be added to make the eye as good a representation of the real eye as possible. Here, we add only the corneal topographic data and set the pupil diameter to 6.0 mm. Pupil diameter and location has a large impact on image quality that is ignored in paraxial calculations but included in exact ray tracings.

For the purposes of our demonstration we correct the model twelve different ways; we correct the eye in the spectacle plane, contact lens plane, corneal plane, and a plane corresponding to an anterior chamber phakic IOL. In each of these correction planes we use three types of correction: a simple

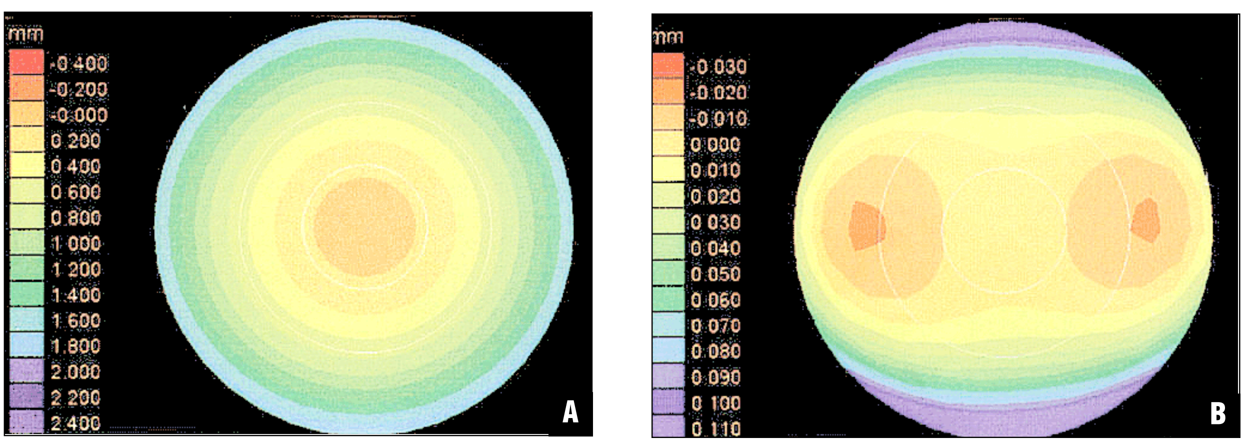

Figure 2. Corneal topography examination elevation **A)** relative to plane, and **B**) relative to ideal conic surface.

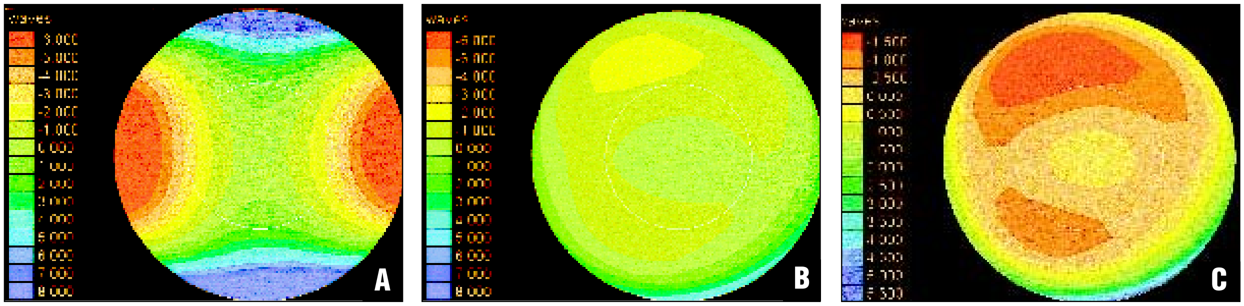

Figure 3. Corneal topography wavefront error **A)** using all Zernike coefficients, and **B)** removing only the Zernike coefficient corresponding to astigmatism in the horizontal or vertical meridian. **C)** Same as (B) but using a different color scale to better show the detail.

Table 2
Zernike Polynomial Coefficients for Corneal First Surface Topography Examination Wavefront Error

N	n	m	Coeff (waves)	Sum Var (waves^2)	Percent Var	Radial Poly
0	0	0	-0.3036	0.0922	0.45	1^(1/2) (1)
1	1	-1	-0.6360	0.4966	1.98	4^(1/2) (1p) sin(t)
2	1	1	0.2581	0.5633	0.33	4^(1/2) (1p) cos(t)
3	2	-2	-0.0853	0.5705	0.04	6^(1/2) (1p^2) sin(2 t)
4	2	0	0.4732	0.7945	1.10	3^(1/2) (2p^2 -1)
5	2	2	-4.3800	19.9785	94.05	6^(1/2) (1p^2) cos(2 t)
6	3	-3	-0.0001	19.9785	0.00	8^(1/2) (1p^3) sin(3 t)
7	3	-1	-0.2550	20.0436	0.32	8^(1/2) (3p^3 -2p) sin(t)
8	3	1	0.0577	20.0469	0.02	8^(1/2) (3p^3 -2p) cos(t)
9	3	3	-0.1898	20.0829	0.18	8^(1/2) (1p^3) cos(3 t)
10	4	-4	-0.0119	20.0830	0.00	10^(1/2) (1p^4) sin(4 t)
11	4	-2	-0.0180	20.0834	0.00	10^(1/2) (4p^4 -3p^2) sin(2 t)
12	4	0	0.5268	20.3609	1.36	5^(1/2) (6p^4 -6p^2 +1)
13	4	2	-0.1819	20.3940	0.16	10^(1/2) (4p^4 -3p^2) cos(2 t)
14	4	4	0.0567	20.3972	0.02	10^(1/2) (1p^4) cos(4 t)
15	5	-5	0.0012	20.3972	0.00	12^(1/2) (1p^5) sin(5 t)
16	5	-3	-0.0003	20.3972	0.00	12^(1/2) (5p^5 -4p^3) sin(3 t)
17	5	-1	-0.0162	20.3975	0.00	12^(1/2) (10p^5 -12p^3 +3p) sin(t)
18	5	1	-0.0182	20.3978	0.00	12^(1/2) (10p^5 -12p^3 +3p) cos(t)
19	5	3	0.0089	20.3979	0.00	12^(1/2) (5p^5 -4p^3) cos(3 t)
20	5	5	0.0082	20.3980	0.00	12^(1/2) (1p^5) cos(5 t)
21	6	-6	0.0013	20.3980	0.00	14^(1/2) (1p^6) sin(6 t)
22	6	-4	0.0026	20.3980	0.00	14^(1/2) (6p^6 -5p^4) sin(4 t)
23	6	-2	-0.0005	20.3980	0.00	14^(1/2) (15p^6 -20p^4 +6p^2) sin(2 t)
24	6	0	0.0206	20.3984	0.00	7^(1/2) (20p^6 -30p^4 +12p^2 -1)

spherical correction, a sphero-cylindrical correction, and high order b-spline correction. For each correction type, the correcting surface is optimized automatically by adjusting the surface parameters to minimize the Stiles-Crawford RMS spot size error defined by equation (1).

$$SC\ RMS = \sqrt{\frac{\sum_{i=0}^{N-1} w_i\left[(x_i - x_c)^2 + (y_i - y_c)^2\right]}{\sum_{i=0}^{N-1} w_i}} \qquad (1)$$

In this equation, the RMS spot size is the root-mean-square radial size. To compute the RMS spot size, the distance between the chief ray's retinal intersection point (x_c, y_c) and each other ray's ultimate location on the retina (x_i, y_i) is squared, and averaged over all rays. The square root of the average is the RMS spot size. To weight the calculation for the Stiles-Crawford effect, we multiply each of the distance-squared values by the SC weight w_i (a value between 0 and 1) and then divide by the sum of the weights for all rays. In the following, the

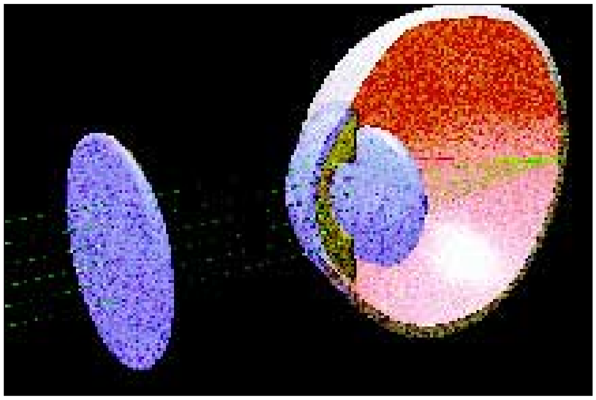

Figure 4. Ray tracing of spherical spectacle lens corrected eye model.

units of SC RMS are in mm, unless otherwise stated.

Spectacle Lens Correction

To model the spectacle lens, we selected a spectacle lens back vertex distance (the distance from the back side of the spectacle lens to the corneal first surface) of 13.0 mm. We set the thickness of the spectacle lens at 1.0 mm, and used optical crown glass as the fabrication material (index of refraction 1.532). For purposes of demonstration, the shape of the lens is plano-concave and we optimized the posterior surface for each surface type (sphere, spherocylinder, and B-spline). The optimized spherical lens was found to have a power of 3.72 D, the spherocylindrical lens was found to be 2.19 D @ 1° x 5.48 D @ 91°. The optimized b-spline surface is represented as a two-dimensional set of control point values that do not have familiar ophthalmic descriptors, but can be visualized as points controlling the shape of the surface such that the SC RMS is minimized.

A six-ray vertical fan ray trace of the spherical surface spectacle lens is shown in Figure 4. Similar ray trace displays can be generated for the other models as well but in the interest of space are not shown. In Figure 5 we show spot diagrams for the uncorrected eye model and the three spectacle corrected eye models. From this figure, we see that as the order of the correction increases (sphere to sphero-cylindrical to b-spline) the optical error indicated by the spot diagram decreases. The SC RMS values for correction with these three surface types is given in the Table 3 also indicating reduced error as the order of correction increases.

From the SC RMS spot size alone, it is often difficult for the user to get a feel for the actual quality of the retinal image. This is particularly true for new users. To enable the user to visualize the optical defects that each model imparts to the retinal image, it is useful to compare simulated retinal images projected into object space. These retinal image simulations are based on linear systems theory for incoherent light transmission through an optical system. The two numerically equivalent

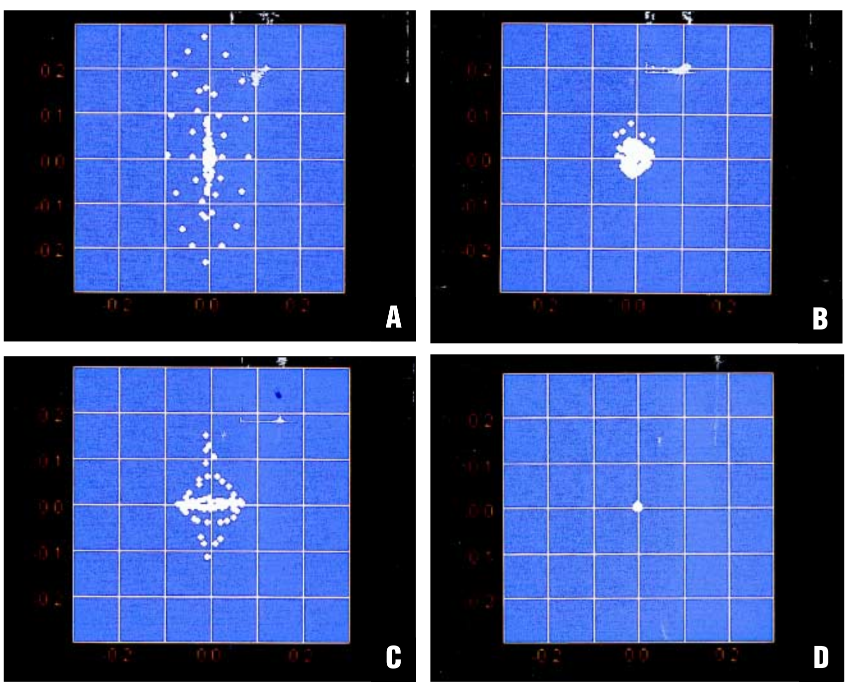

Figure 5. Spot diagrams for **A)** uncorrected eye model and **C)** spectacle lens corrected eye models with spherical back surface, **B)** spherocylindrical back surface, and **D)** b-spline back surface.

Table 3
Comparison SC RMS (mm) for Various Corrections With Various Type Surfaces*

Correction Surface	Spectacle	Contact Lens	Cornea	Phakic IOL
Sphere	0.0506	0.0291	0.0500	0.0501
Sph/Cyl	0.0303	0.0267	0.0500	0.0284
B-Spline	0.0012	0.0003	0.0001	0.0027

*For comparison, the Schwieglerling eye in its native state with a 6.0 mm pupil has an SC RMS of 0.028.

methods to compute the simulated retinal image are (1) to compute the convolution of the input image with the point spread function of the optical system, and (2) to compute the discrete Fourier transform (DFT) of the input image and the point spread function, perform a point-wise complex multiplication, and then compute the inverse DFT of the result. To speed up the calculations, fast Fourier transforms (FFTs) are employed to compute the DFTs. Figure 6 shows a comparison of the simulated retinal image for the uncorrected eye model and the three spectacle corrected eye models. As with the spot diagram, there is a subjective improvement in the quality of the image as the order of the surface correction increases.

Contact Lens Correction

The corneal topography examination has simulated keratometry values of 44.75 @ 91° x 42.42 @ 1°, revealing astigmatism of about 2.33 D. For our hypothetical contact lens we selected a toric base curve with principal meridians that were about 0.25 D flatter than the corneal surface meridians (Table 10.3 in reference #3). This leads to back surface radii of 8.0 and 7.58 mm. Other lens specifications are center thickness of 0.28 mm, PMMA material with index of refraction of 1.492, and tears with index of refraction of 1.336. For this example, we assumed the contact lens would center on the eye's pupil. Under these conditions, the surface to be optimized is the contact lens front surface. The SC RMS values for correction with the three surface types are given in Table 3. Notice that the difference between the spherical front surface and the spherocylindrical front surface SC RMS values is small, demonstrating the effects of tear lens and the toric back surface of the contact lens.

Correction at Anterior Cornea

It was previously demonstrated that the anterior cornea of our model contains significant low and high order aberrations. If we now return to the initial parameters of the Schwiegerling model with a 6.0 mm pupil, we can compare the SC RMS error in the initial model with the error for a spherical anterior cornea and the optimal b-spline corneal surface (Table 3). Since we optimize using the SC RMS value, a corneal first surface sphere and spherocylinder will lead to the same result. Note that the SC RMS error value increased significantly from 0.028 to 0.050 as we moved from the aspheric model parameter to a spherical (or sphero-cylindrical) anterior cornea, but dropped to 0.0001 for the b-spline surface. Also note that the error in the

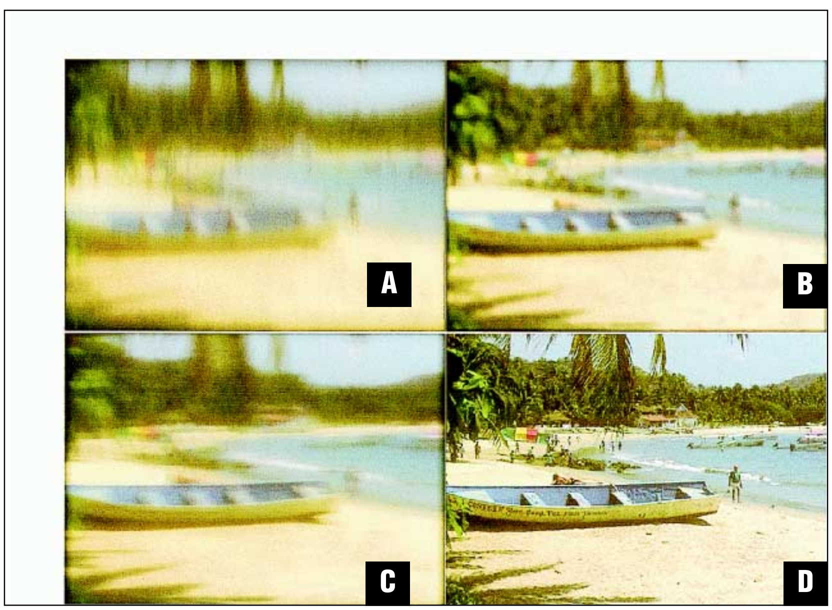

Figure 6. Retinal image simulation for **A)** uncorrected eye model and spectacle lens corrected eye models with **(C)** spherical back surface, **(B)** spherocylindrical back surface, and **(D)** b-spline back surface.

initial Schwiegerling eye model (SC RMS = 0.028) is present by design to mimic the naturally occurring optical aberration in human eyes.

Anterior Chamber Phakic IOL

For our anterior chamber phakic IOL example, we located the back vertex of the lens just anterior to the iris plane and specified an index of refraction of 1.4915 (PMMA in situ). The optic diameter is 6.0 mm and the center thickness is 0.5 mm. The shape of the lens is plano-concave and for our comparison we varied the back surface of the lens, leaving the first surface fixed. Values for SC RMS error for the three surface types are given in Table 3. Note that in this case the B-spline SC RMS value is 2.7 µm, which is twice the SC RMS value (1.2 µm) for the B-spline spectacle lens. This difference is due to the numerical tolerance in the automatic surface optimization routine and has negligible effect on the simulated retinal image.

DISCUSSION

The overall goal of the VOL-3D project is to develop for clinical and research use, a user-friendly software program which models and evaluates the optics of a real and/or user-defined eye and stores analysis outcomes in a relational database. Our approach is to streamline the modeling, optimization, and analysis tasks by developing a single integrated program written in the language of visual optics. We illustrate our progress here by demonstrating how the program can use clinical data to develop an optical model of a patient's eye and evaluate various corrections designed to improve retinal image quality.

REFERENCES

1. Grievenkamp JE, Schwiegerling J, Miller JM, Mellinger MD. Visual acuity modeling using optical raytracing of schematic eyes. Am J Ophthalmol 1995;120:227-240.
2. Schwiegerling J. Optical modeling of radial keratotomy incision patterns. Am J Ophthalmol 1996; 122:808-817.
3. Mandell RB. Contact Lens Practice, 4th edition. Boston, MA: Charles C Thomas Publisher, 1988.